JOURNAL OF GEOPHYSICAL RESEARCH, VOL. 102, NO. D11, PAGES 13,291–13,299, JUNE 20, 1997

Biomass burning and deep convection in southeastern Asia: Results from ASHOE/MAESA

Ian Folkins
Atmospheric Science Program, Departments of Physics and Oceanography, Dalhousie University Halifax, Nova Scotia, Canada

R. Chatfield
Earth System Science Division, NASA Ames Research Center, Moffett Field, California

D. Baumgardner
Atmospheric Technology Division, National Center for Atmospheric Research, Boulder, Colorado

M. Proffitt
NOAA Aeronomy Laboratory and Cooperative Institute for Research in Environmental Sciences Boulder, Colorado

Abstract. There was extensive biomass burning in Indonesia, northern Australia, and New Guinea during September and October 1994. This paper discusses two accidental encounters of biomass plumes from the 1994 Airborne Southern Hemisphere Ozone Experiment and Measurements for Assessing the Effects of Stratospheric Aircraft campaign (ASHOE/MAESA). During the October 23 descent into Fiji, and an ascent from Fiji on October 24, the NASA ER-2 passed through layers highly enhanced in NO, NO_y, CO, and O_3. These layers occurred near an altitude of 15 km. Back trajectories and satellite images indicate that the layers probably originated as outflow from a convective disturbance near New Guinea. The measurements indicate that deep convection can inject emissions from southeast Asian biomass burning to near tropical tropopause altitudes. Deep convection magnifies the impact of biomass burning on tropospheric chemistry because of the much longer residence times and chemical lifetimes of species in the upper tropical troposphere. Transport of the products of southeast Asian biomass burning into the upper tropical troposphere, followed by southward high-level outflow and advection by the subtropical jet, may play a significant role in dispersing these emissions on a global scale. Anthropogenic emissions from countries in southeast Asia are likely to increase in the future as these countries become more highly industrialized. This transport mechanism may play a role in increasing the impact of these types of emissions as well.

1. Introduction

There are strong seasonal and geographic variations in the chemical composition of the tropical troposphere. Much of this variability is caused by emissions from biomass burning. The largest burning-induced perturbations of the tropical atmosphere are probably in the South Atlantic [*Fishman et al.*, 1990], where anomalously high tropospheric ozone concentrations are known to be largely due to seasonal burning in southern Africa and South America [*Logan and Kirchhoff*, 1986; *Andreae et al.*, 1994]. At the other extreme is the mid-equatorial Pacific, where the dominant mode of air input into the upper troposphere is deep convection over the ocean, and the influence of biomass burning appears to be much less [*Crutzen and Andreae*, 1990]. Air in this region is usually very pristine, with ozone mixing ratios typically less than 25 ppbv [*Routhier and Davis*, 1980; *Fishman et al.*, 1987; *Kley et al.*, 1996], and NO mixing ratios less than 20 pptv [*McFarland et al.*, 1979; *Ridley at al.*, 1987; *Folkins et al.*, 1995; *Davis et al.*, 1996; *Singh et al.*, 1996].

Although biomass burning does occur in southeast Asia, the extent to which these fires influence the photochemistry of the surrounding region is much less well characterized than those which occur in South Amer-

Paper number 96JD03711.
0148-0227/97/96JD-03711$09.00

ica and southern Africa. Burning occurs annually in parts of Indonesia prior to and during the months of September and October [*Bachmeier et al.*, 1996]. However the strength and timing of burning in Indonesia and northern Australia appears to be strongly modulated by the El Nino Southern Oscillation (ENSO). Large sections of the rain forest in Borneo burned in the early months of 1983 as a result of ENSO-related drought conditions [*Malingreau et al.*, 1985]. These fires were probably responsible for the large increases in total column ozone observed above Indonesia at this time by the total ozone mapping spectrometer (TOMS) [*Fishman et al.*, 1990]. During the October 13 flight of the 1991 Pacific Exploratory Mission (PEM) West A campaign, the DC-8 intercepted a plume highly enhanced in a variety of chemical species including ethane [*Bachmeier et al.*, 1996] and peroxides [*Heikes et al.*, 1996]. This plume was attributed to burning in Borneo, again due to below normal rainfall associated with the ENSO phase.

There was extensive biomass burning throughout Indonesia, New Guinea, and northern Australia in September, October, and November 1994. The extensive low-level haze produced by these fires gave rise to severe air quality problems in Singapore and Malaysia. This haze was observed by astronauts on the Space Shuttle Atlantis. The Space Shuttle photograph with image number STS066-154-157 (not shown), taken on November 14, 1994, shows the islands of Java, Bali, and Lombok. The description accompanying this photo reads in part, "The region appears hazy due to extended drought over Indonesia and Australia. Because of drought conditions, huge fires continue to burn over other regions of Indonesia, New Guinea and northern Australia, producing a regional smoke pall."

The southeast Asian fires of 1994 emitted large quantities of carbon monoxide (CO). Atlantis carried the MAPS (measurement of air pollution from satellites) instrument designed to measure tropospheric CO. A compilation of the CO measurements taken using this instrument between September 30 and October 11 1994 [*Connors*, 1997] show CO enhancements in South America and southern Africa. These enhancements presumably reflect the biomass burning usually occurring in these regions at this time of year. Unlike previous years however [*Connors*, 1991], there was also an extensive region of CO enhancement in the eastern Indian Ocean, and over Indonesia and northern Australia. This region of elevated CO appears more extensive in size than either of the elevated CO regions in South America or southern Africa, and suggests that tropical biomass burning emissions in 1994 may have been dominated by fires in southeast Asia.

Significant enhancements in total ozone above Indonesia were observed in September and October 1994 by both the Meteor3/TOMS instrument and ground-based Brewer total ozone measurements [*Fujiwara et al.*, 1996]. Figures released by the Indonesian Ministry of Forestry indicate that a land area of about 5.1 million hectares was affected by fires in 1994 [*Goldammer et al.*, 1996]. Most of this burning was associated with farming activities and occurred in Kalimantan and Sumatra. These fires were due in part to ENSO-related drought conditions. There were pronounced negative deviations in the southern oscillation index (SOI) during this period, as well as positive sea level pressure (SLP) anomalies over Indonesia and Australia [*Kousky*, 1994].

Measurements from Brazil and southern Africa during the 1992 TRACE A (Transport and Atmospheric Chemistry near the Equator - Atlantic) have demonstrated that deep convection can transport ozone precursors into the upper troposphere [*Thompson et al.*, 1996, *Pickering et al.*, 1996]. Warm sea surface temperatures help give rise to extremely vigorous deep convection in the western equatorial Pacific [*Danielsen*, 1993]. The injection of southeast Asian biomass burning emissions into the upper troposphere by deep convection would be expected to magnify their impact on tropospheric photochemistry [*Chatfield and Crutzen*, 1984; *Dickerson et al.*, 1987; *Chatfield and Delany*, 1990; *Pickering et al.*, 1990, 1992]. Mechanisms through which this occurs include the following. First, upper level winds are usually much stronger than those near the surface, so that convection helps spread and dilute emissions over a much larger area. Second, on a per molecule basis, NO_x from fires can be expected to produce more ozone in the upper troposphere than near the surface. This is due partly to the fact that timescales for oxidation of NO_x to HNO_3 are much longer in the upper troposphere than near the surface. The lifetime of NO_x with respect to oxidation by OH increases from a few days in the boundary layer to a week or more in the upper equatorial Pacific troposphere [*Folkins et al.*, 1995; *Davis et al.*, 1996]. This increase with height is due largely to the higher NO/NO_2 ratios of the upper troposphere, which slow down the NO_2 + OH reaction rate. Once oxidized to HNO_3, reactive nitrogen in the boundary layer is rapidly removed via surface deposition and washout. In the upper tropical troposphere, timescales for rainout and washout are much longer [*Giorgi and Chameides*, 1986], and photolysis of HNO_3 is sufficiently fast that NO_x can be recycled from HNO_3 and produce additional ozone. Third, ozone is a greenhouse gas whose radiative forcing is largest in the upper troposphere where temperatures are coldest [*Lacis et al.*, 1990]. Deep convection can therefore enhance the climatic effects of biomass burning.

2. ER-2 Measurements

During the 1994 Airborne Southern Hemisphere Ozone Experiment and Measurements for Assessing the Effects of Stratospheric Aircraft (ASHOE/MAESA) campaign [*Tuck et al.*, 1997], there were a number of ferry flights between the main operational base in Christchurch New Zealand, and NASA Ames in California. As part of its

final return to Ames, the ER-2 flew from Christchurch to Fiji on October 23, 1994. It left Fiji for Hawaii on October 24. The ER-2 is a heavily instrumented aircraft with a cruising altitude of 18-20 km.

Nitrous oxide (N_2O) was measured from the ER-2 during ASHOE/MAESA [*Podolske and Loewenstein*, 1993], and its variation with height during the October 23 descent into Fiji is shown in Figure 1. N_2O sharply decreases above 90 mbar but is nearly uniform below 90 mbar. One would therefore expect the tropopause to occur near 90 mbar. This corresponds to a potential temperature of 385 K. This definition is consistent with the temperature profile shown in Figure 7, which shows that the temperature minimum occurs at 90 mbar as well.

Figure 1 also shows total reactive nitrogen (NO_y) during the October 23 ER-2 descent into Fiji [*Fahey et al.*, 1989]. Within the troposphere (below 90 mbar), there are two layers of anomalously high NO_y. The upper layer occurs between 110 and 140 mbar (approximately 14-16 km) and the lower layer occurs between 420 and 580 mbar. In both cases, NO_y mixing ratios considerably exceed the 200 pptv typically observed in the equatorial Pacific upper troposphere [*Folkins et al.*, 1995].

The main source of NO_y in the stratosphere is the reaction of N_2O with O^1D, which produces two NO radicals. This reaction helps give rise to the well-known anticorrelation between NO_y and N_2O in the stratosphere [*Loewenstein et al.*, 1993]. The top panel of Figure 1 shows NO_y plotted against N_2O during the October 23 ER-2 descent. Within the stratosphere, these points project onto a single line. The points within the upper enhanced NO_y layer, having NO_y mixing ratios of 1000 pptv and N_2O mixing ratios of 311 ppbv, strongly deviate from the overall linear relationship. This indicates that the stratosphere can be discounted as the source of the enhanced NO_y in this layer. Unfortunately, the absence of N_2O measurements in the lower layer makes it difficult to determine if this NO_y enhancement is stratospheric or tropospheric in origin.

Figure 2 shows measurements of NO [*Fahey et al.*, 1989], CO [*Webster et al.*, 1993, 1994], O_3 [*Proffitt et al.*, 1989] and total H_2O [*Kelly et al.*, 1990] during the October 23 descent. The upper layer of enhanced NO_y in Figure 1 coincides with enhancements in NO, CO, and O_3. The CO enhancement provides additional evidence that the layer is not of stratospheric origin. NO mixing ratios of about 300 pptv within the layer are about an order of magnitude higher than background values. NO_y variations in the lower layer are positively correlated with O_3 and negatively correlated with H_2O.

The chemical anomalies observed on October 23 were still present 36 hours later when the ER-2 left Fiji for Hawaii. Measurements of NO, CO, O_3, and H_2O during the October 24 ascent from Fiji are shown in Figure 3. There are continued strong enhancements in CO, NO, and O_3 between 100 and 130 mbar. O_3 and H_2O remain anticorrelated in the lower layer between 420 and 580 mbar.

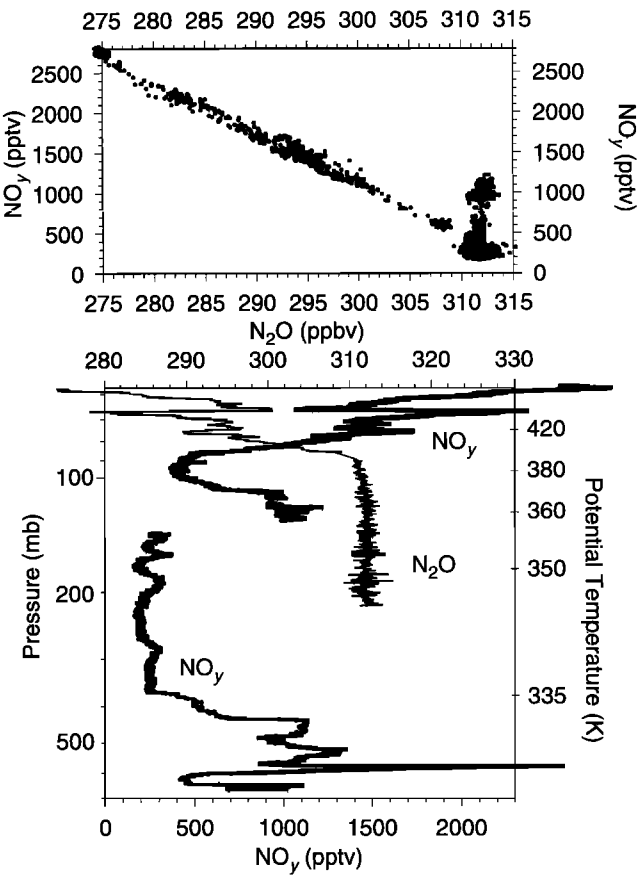

Figure 1. (top) Scatterplot of NO_y versus N_2O during the October 23 descent into Fiji. (bottom) Plot of NO_y and N_2O versus pressure during the descent. The points most strongly deviating from linearity in the scatterplot come from the 110 - 130 mbar interval in the vertical profile.

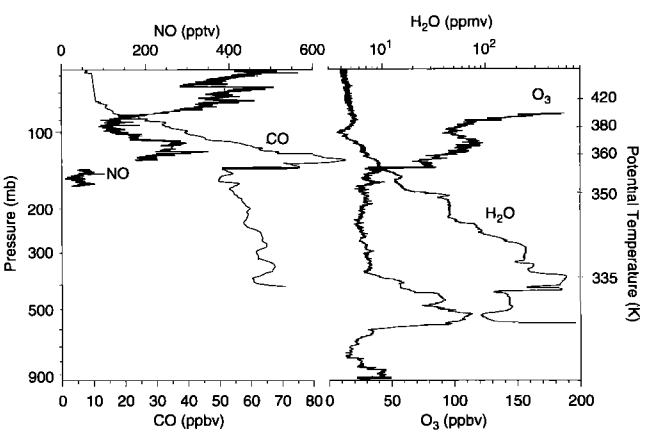

Figure 2. NO, CO, H_2O, and O_3 during the October 23 ER-2 descent into Fiji. Note the enhanced NO, CO, and O_3 between 110 and 140 mbar, and the O_3 - H_2O anticorrelations between 420 and 580 mbar.

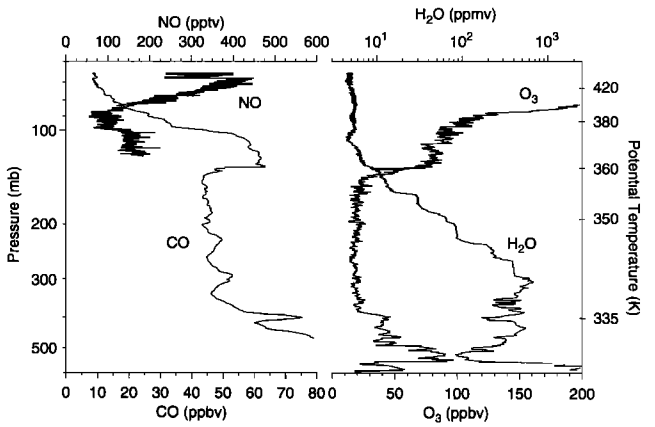

Figure 3. NO, CO, O_3, and H_2O during the October 24 ER-2 ascent from Fiji. Note the enhanced CO and NO still present in the upper troposphere.

3. Back Trajectories and Satellite Images

Figure 4 shows a cluster of 10 day back trajectories originating from the vicinity of the October 23 upper NO_y layer. The trajectories are isentropic with a common potential temperature of 365 K. In the absence of condensational heating or evaporative cooling, potential temperature is nearly conserved on a timescale of several days, especially near the tropical tropopause where heating rates are small (see Figure 7). The assumption of constant potential temperature should therefore be reasonably well obeyed in the absence of cloud processes. The back trajectories shown in Figure 4 were calculated using the Goddard Space Flight Center (GSFC) Trajectory Model [*Schoeberl and Sparling*, 1994] with winds from an assimilation scheme (ASM). There are two types of trajectories originating from near the upper NO_y layer. The largest group of trajectories starts above the equator, proceeds toward the west, and then comes back to Fiji after reversing direction between Australia and New Guinea. The other group is more localized near Fiji.

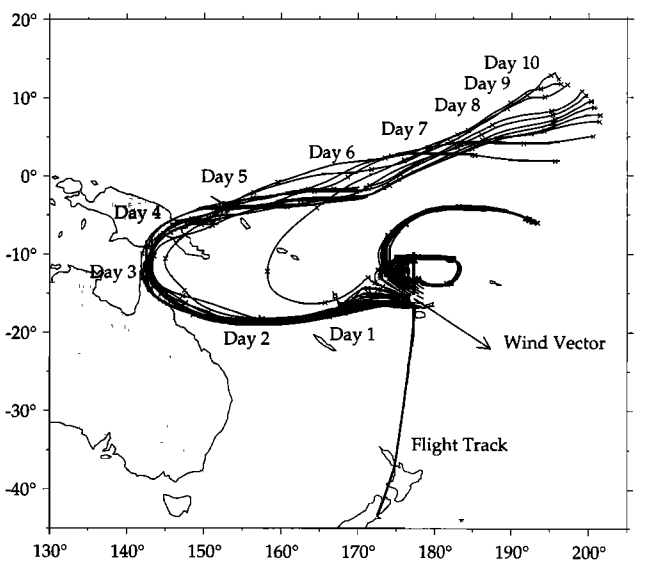

Figure 4. Isentropic 10 day back trajectories from points clustered about the location of the ER-2 descent into Fiji. The common 365 K potential temperature of the trajectories is near the midpoint of the upper NO_y layer in Figure 1. Crosses along the trajectories separate 1 day intervals. The ER-2 flight track from Christchurch to Fiji has been drawn in as a thick line. The arrow denotes the direction of the 365 K wind vector as measured from the ER-2.

Figure 5 shows visible and infrared AVHRR (advanced very high resolution radiometer) images of eastern Australia and New Guinea taken at 2051 UT on October 19, 3.25 days prior to the ER-2 descent on October 23. The eastern coastline of Australia can be seen in the visible image. Figure 6 shows the domain of the two satellite images. A prominent feature of both is the midlatitude cyclone centered near Tasmania. There is also a site of deep convective near the top of the images just off the eastern coast of New Guinea. This surface low would give rise to an upper level anticyclonic (anticlockwise in the southern hemisphere) circulation in the upper troposphere. It appears to be associated with the reversal in direction of the larger of the two groups of trajectories shown in Figure 4.

The back trajectories of Figure 4 and satellite images of Figure 5 are consistent with the notion that air within the upper NO_y layer in Figure 1 originated 3-4 days earlier as outflow from a deep convective site near New Guinea. The extensive biomass burning occurring at this time in Indonesia, northern Australia, and New Guinea is the most plausible explanation for the large CO enhancements of this layer. A back trajectory cluster calculated using winds from the United Kingdom Meteorological Office (UKMO) is very similar to the group of trajectories shown in Figure 4 which traverse New Guinea and Australia. The UKMO trajectories give no indication of the small scale circulation which gives rise to the more localized ASM trajectories in Figure 4. Assimilation models do however often perform poorly in the tropics due to a lack of observational data. Some comparisons of winds in the tropics observed from the ER-2 during ASHOE/MAESA with forecast and assimilated winds are given by *Tuck et al.* [1997]. The in situ wind vector measured from the ER-2 at 365 K is drawn in Figure 4. Its direction is roughly consistent with the direction of the back trajectories.

The ASM winds have also been used to calculate the 10 day back trajectory starting from the upper layer of enhanced NO and CO on October 24. The shape of this trajectory is very similar to the group of trajectories shown in Figure 4 traversing northern Australia and New Guinea. This indicates that the upper layers of anomalously high NO and CO seen on October 23 and 24 probably originate from the same deep convective system.

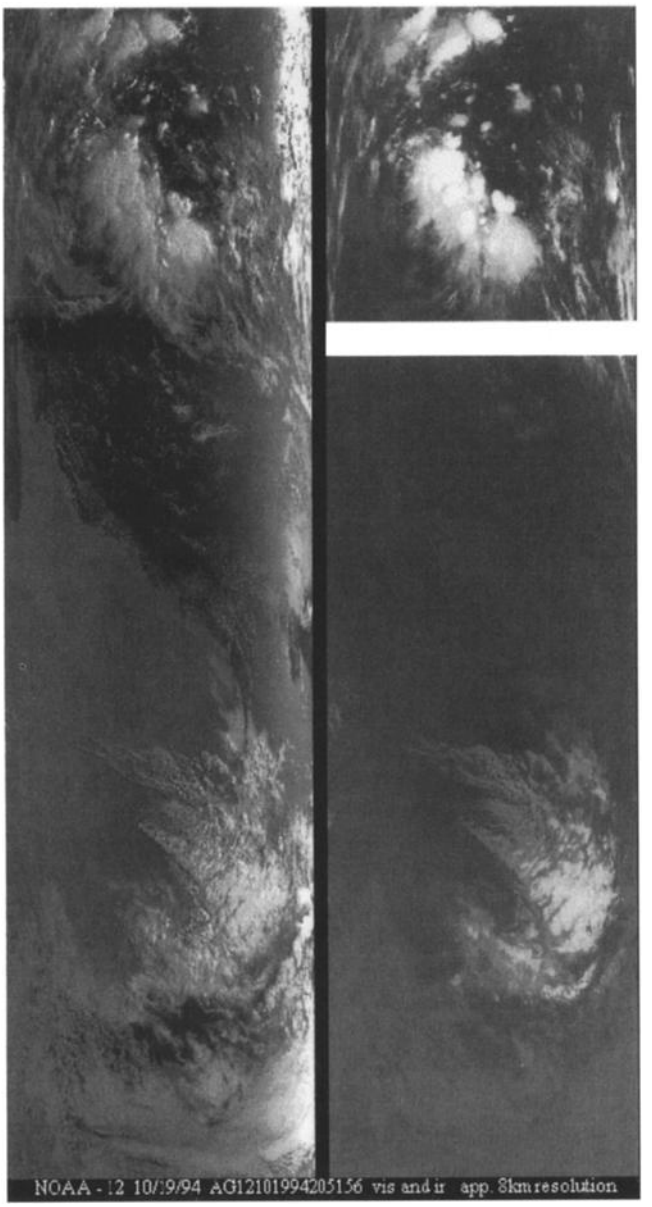

Figure 5. (left) Visible and (right) infrared AVHRR images of eastern New Guinea and Australia at 2051 UT on October 19, 1994. Note the convective cloud cluster near the top of the images, and the midlatitude cyclone near the bottom. The outlines of Australia and New Guinea can be seen in the visible image.

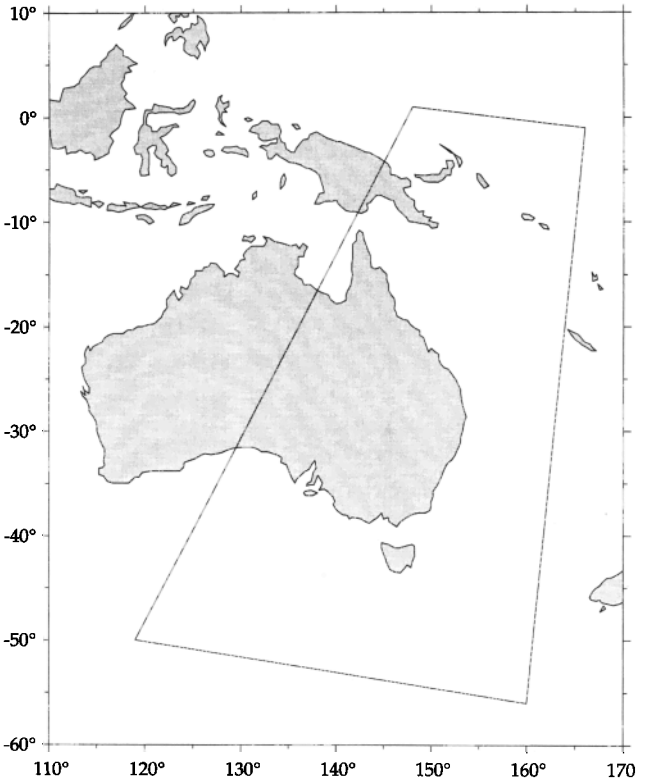

Figure 6. Domain of the October 19, 1994 AVHRR images shown in Figure 5.

4. Enhancement Ratios

Emissions from biomass burning give rise to characteristic relative enhancements of chemical species. These enhancements are ordinarily indexed against CO_2. *Andreae* [1991] gives best guess emission ratios for CO and NO_x of $\Delta CO/\Delta CO_2 \sim 0.1$ and $\Delta NO_x/\Delta CO_2 \sim 0.0021$. Combining these two ratios gives $\Delta NO_x/\Delta CO \sim 0.021$. Emission ratios vary dramatically depending on the fire stage and nitrogen content of the fuel [*Lobert*, 1991]. Enhancement ratios within plumes will evolve with time as air within the plume is mixed with background air characterized by differing relative concentrations of species, as CO is oxidized to CO_2, and as NO_x is converted to other forms of reactive nitrogen, some of which will be soluble and therefore subject to washout and rainout. Ozone enhancements within the plume (shown in Figure 2) indicate that some oxidation of CO to CO_2 has already taken place. After detrainment, NO_y is a more conservative tracer than NO_x and therefore probably gives a better indication of the NO_x originally emitted into the plume. The NO_y enhancement of the upper layer in Figure 1 is roughly constant at 500 pptv. The CO enhancement within the layer varies from near zero to 35 ppbv. One can roughly estimate a CO enhancement of 30 ppbv by assuming that the largest CO enhancements are more likely to be representative of the actual CO enhancement due to biomass burning. This yields an enhancement ratio of $\Delta NO_y/\Delta CO \sim 0.017$. This is quite close to the ratio $\Delta NO_x/\Delta CO \sim 0.021$ given above and supports the notion that the NO_y enhancements within the layer do originate from biomass burning.

5. Clear Sky Radiative Heating Rates

The extent to which deep convection contributes to the global dispersal of the products of biomass burning depends in part on the altitude of detrainment. Emissions which detrain at higher altitudes will in general

have longer residence times, and be transported longer distances, than emissions which detrain closer to the surface. The residence time of an air parcel in the upper tropical troposphere will be partly determined by the heating rate vertical profile. Large-scale downward motion in the tropics occurs via subsidence associated with radiative cooling. Air parcels which detrain near the tropical tropopause might be expected to have particularly long residence times because clear sky heating rates go from negative in the troposphere (net cooling) to positive in the stratosphere (net heating).

The ER-2 measurements of temperature, ozone, water vapor, and pressure during the October 23 descent have been used as inputs into a one-dimensional radiative transfer model to calculate the clear sky heating rate vertical profile. The radiative transfer model is based on the δ-four-stream method [*Liou et al.*, 1988], and employs the correlated k-distribution technique for gaseous absorption and emission [*Fu and Liou*, 1992]. It was formulated on pressure levels with a spacing of 1 mbar near the tropopause. The cosine of the solar zenith angle was fixed at 0.5 to approximate a diurnal average. This choice does not strongly affect heating rates near the tropopause, which are dominated by contributions from the longwave portion of the spectrum.

The total (solar + longwave) clear sky heating rates generated by the model are shown in Figure 7. The first onset to positive net heating occurs considerably below the tropopause (90 mbar), and close to the bottom of the plume at 140 mbar. The near zero clear sky heating rates within the plume suggest very slow subsidence, and enhance the likelihood of very long range transport.

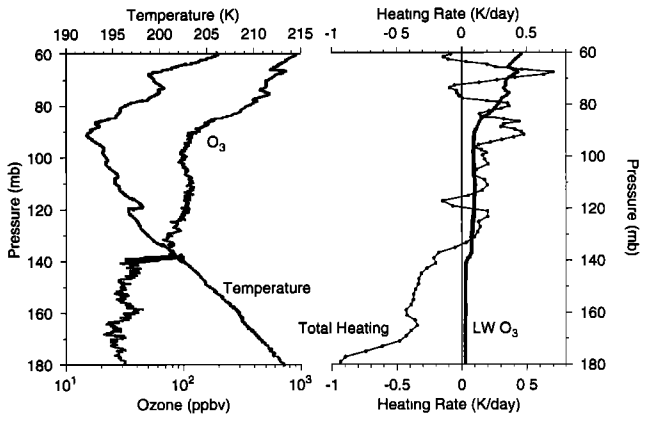

Figure 7. (left) Temperature and ozone, as measured from the ER-2 during the October 23 descent into Fiji, between 60 and 180 mbar. (right) Total (solar + longwave) clear sky heating rate versus pressure as calculated by a radiative transfer model using as inputs the ER-2 measurements of temperature, pressure, ozone, and water vapor. The contribution of the 9.6 μm ozone band to the total heating is shown as a thick line. Note the strong anticorrelation between temperature and heating rate near the tropopause. Photon path lengths in the 15 μm band of CO_2 are sufficiently short that positive temperature fluctuations are rapidly damped by negative heating rates, and vice versa.

Heating rates near the tropopause are largely a residual between cooling associated with water vapor emission, and warming associated with net longwave absorption by the 15 μm CO_2 band. Figure 7 also shows that longwave heating by the 9.6 μm ozone band within the plume (110-140 mbar) does help shift this residual toward positive net heating. This suggests that ozone production within biomass-burning plumes near the tropical tropopause may lengthen their residence times by contributing toward radiative self-lofting.

It should be noted that clear sky radiative heating rates can be drastically altered by the presence of clouds. Cloud top cooling rates are of the order of 10 K/d. The addition of a cloud below the plume would largely absorb the warm upwelling radiation from the surface and sharply diminish longwave ozone heating within the plume. It would not, however, change the overall shape of the clear sky radiative heating rates shown in Figure 7 or strongly perturb heating rates within the plume from their near zero values.

6. Aerosol Volume and Ozone Profiles

Biomass burning affects the radiative forcing at the surface primarily through the emission of black carbon, aerosol-forming sulfur compounds, and ozone precursors. Aerosol concentrations in various size bins were measured from the ER-2 using a multiangle aerosol spectrometer probe (MASP) [*Baumgardner et al.*, 1996]. Aerosol volume was obtained by integrating over size bins from 0.15 to 10 μm. Its variation with height during the October 23 descent into Fiji is shown in Figure 8. Aerosol volumes are higher in the stratosphere (above 90 mbar), within the dry, ozone rich layer between 420 mbar and 580 mbar, and below 850 mbar in the ma-

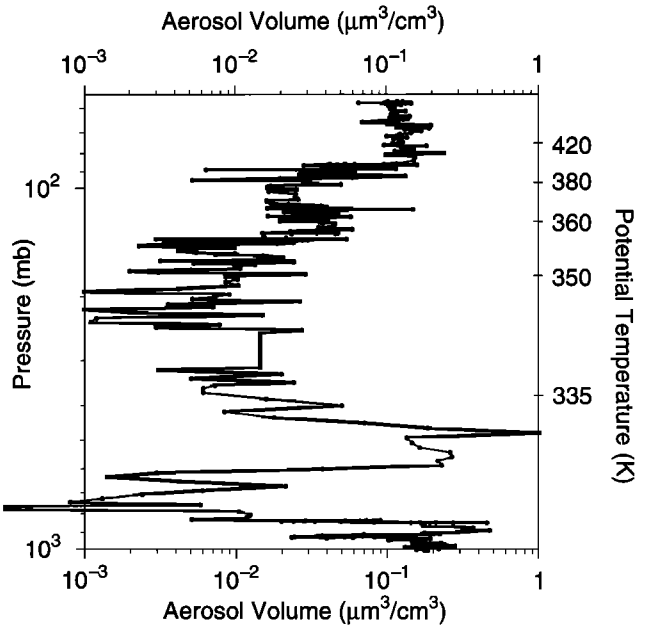

Figure 8. Aerosol volume versus pressure during the October 23, 1994, descent into Fiji.

rine boundary layer. They are also somewhat enhanced within the 110 to 140 mbar plume interval.

It is possible to estimate the aerosol volume enhancement that would have occurred if none of the sulfate aerosol within the plume had been removed during deep convection. Using a CO enhancement within the plume of 30 ppbv, the SO_x (= SO_2 + aerosol sulfate) emission ratios of *Andreae* [1991], and assuming that all the emitted SO_x is converted to aerosols consisting of 50% by mass H_2O, gives an aerosol volume enhancement of 0.6 $\mu m^3/cm^3$ within the plume. The observed aerosol volume enhancement within the plume is about 0.04 $\mu m^3/cm^3$, more than 10 times smaller than the above estimate. This implies a deep convective removal efficiency of greater than 90%.

Ozone is a greenhouse gas whose radiative forcing strongly depends on altitude. On a per molecule basis, its forcing is strongest at the tropopause [*Lacis et al.*, 1990]. Some indication of the enhancement in upper tropospheric ozone above Fiji caused by southeast Asian biomass burning can be obtained by comparing the ozone profiles above Fiji in October with those 7 months earlier. Figure 9 shows the two October ozone profiles together with two profiles taken in March. The two October profiles show considerable enhancement over those in March between 355 K and 375 K, within the altitude range at which the radiative forcing of ozone is maximized.

Some of the differences in the two sets of profiles in Figure 9 may be due to seasonal variability [*Komala at al.*, 1996]. Stratospheric (above 380 K) O_3 mixing ratios are consistently higher in October than March, despite the fact that ozone mixing ratios at these altitudes are unlikely to have been affected by biomass burning. This

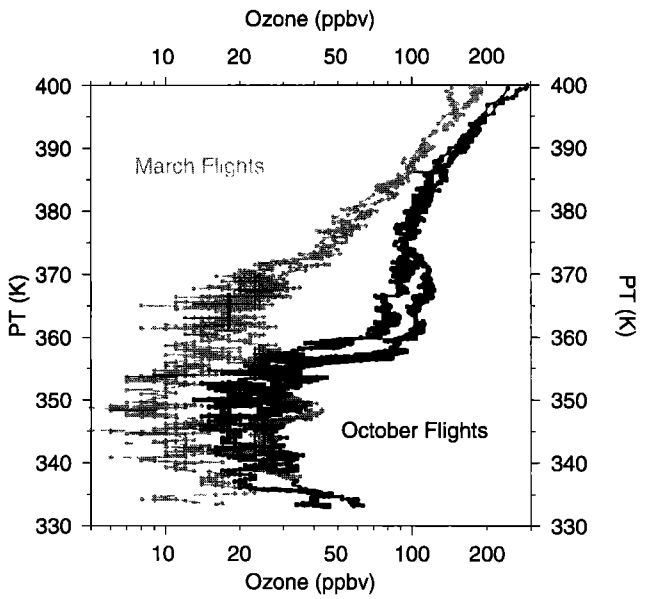

Figure 9. A comparison of the two ozone profiles above Fiji taken during on October 23 and 24, with two profiles taken 7 months earlier on March 27 and 29.

may be because upwelling in the lower stratosphere is strongest during northern hemisphere winter [*Holton et al.*, 1995]. Stronger advection of ozone poor air from below during the winter would tend to reduce O_3 mixing ratios in the lower stratosphere, and may induce a seasonal cycle in which O_3 is lower during northern hemisphere spring than fall.

7. Discussion

Measurements discussed in this paper appear to confirm a prediction by *Goldammer et al.* [1996] that deep convection in southeast Asia can contribute to the global dispersal of biomass burning emissions. This dispersal occurred despite the overall inhibition of deep convection in this region associated with the negative ENSO phase.

The extent to which biomass burning increases ozone production rates in the upper tropical troposphere depends on the extent to which it simultaneously increases both CO and NO concentrations at these altitudes. The upper tropospheric CO enhancements seen on October 23 and 24 are almost certainly due to biomass burning. It is not however possible to rule out lightning [*Tuck*, 1976] as a contributor to the NO_y enhancements. Lightning has been suggested as an important source of NO_y to this region [*Murphy et al.*, 1993], and this appears to be confirmed by recent measurements [*Kawakami et al.*, Impact of lightning and convection on reactive nitrogen in the tropical free troposphere, submitted to *Journal of Geophysical Research*, 1997]. However the uniformity of the NO_y and NO enhancements in the plumes, and the fact that the NO_y enhancement on October 23 was comparable to that anticipated from biomass burning, support the notion that the reactive nitrogen enhancements did originate from biomass burning.

The very dry lower layer of enhanced NO_y, O_3, and CO probably originated from the midlatitude upper troposphere. Well-defined layers with these chemical characteristics are frequently observed in the subtropics and are associated with transport of midlatitude air into the tropics [*Fishman et al.*, 1987, *Danielsen et al.*, 1987]. *Newell* [1996] provides a discussion of layers of this type observed in PEM West A. Five day isentropic back trajectories from this layer originate from central Australia and descend rapidly prior to intersecting the ER-2 flight track. This subsidence is probably related to the midlatitude cyclone near Tasmania seen in Figure 5.

The quasi-isentropic transport of air from midlatitude regions into the tropics by midlatitude cyclones will generally be restricted to isentropic surfaces of 335 K or lower. Because of the shorter residence times of chemical species in the lower troposphere, species such as O_3 and NO_y transported into the equatorial Pacific in this way will have less impact on a per molecule basis than species injected into the upper troposphere by deep convection.

8. Conclusions

Flights from the 1994 ASHOE/MAESA campaign have yielded new insights into the effects of biomass burning in southeast Asia on the chemical composition of the western equatorial Pacific. In situ measurements from this campaign, in conjunction with meteorological analyses and satellite images, have demonstrated that deep convection in southeast Asia can inject emissions from biomass burning to near tropical tropopause altitudes.

Deep convection magnifies the impact of emissions from biomass burning on tropospheric chemistry by spreading out their perturbative effects over increased timescales and spatial scales. The lifetimes of many soluble chemical species, or species such as O_3 which have surface losses, are determined in large part by the timescale required for subsidence and eventual entrainment into the surface boundary layer. This timescale increases from days in the lower troposphere to weeks or months in the upper tropical troposphere. In the case of the biomass-burning plume discussed here, residence times can be expected to be particularly long because clear sky radiative heating rates within the plume were slightly positive. During the 3-4 days since detrainment, the plume had traveled approximately 4000 km from eastern New Guinea to Fiji. A 10 m/s wind and a residence time of a month could easily have given rise to a hemispheric-wide dispersal of the plume.

When coupled with deep convection, biomass burning is a source of O_3 and NO to the upper tropical troposphere, a region which is dynamically inaccessible to the midlatitude troposphere. At present, it is not known how frequently deep convection near Indonesia is able to pump biomass burning emissions into the upper troposphere. An assessment of the global significance of these types of events is therefore not possible. Extensive biomass burning in this region appears to be quasi-periodic rather than annual. The biomass burning in Indonesia and surrounding areas occurring in October and November 1994 was caused by a drought instigated by an El Nino. This is consistent with previous reports of biomass burning in this region. However, anthropogenic emissions from southeast Asia are expected to increase in the future as the countries in this region become more highly industrialized. The dynamical mechanism discussed in this paper would also apply to the dispersal of these types of emissions.

Acknowledgments. We thank the large number of people who made the ASHOE/MAESA measurements possible. In particular, we thank D. Fahey for NO_y and NO, C.R. Webster and R. D. May for CO, K. Kelly for H_2O, M. Loewenstein and J. Podolske for N_2O, and K. R. Chan for temperature and pressure. We also thank D. P. McNamara, G. Morris, and L. R. Lait of the NASA/Goddard Space Flight Center for back trajectories. Comments on the draft by A. F. Tuck and A. M. Thompson led to significant modifications and improvements of the manuscript. We are also grateful to Q. Fu for the use of his radiation code, to R. Yokelson for his insights on the Indonesian fires of 1994, and to R. Slack of Resonance Ltd. for bringing the MAPS images to our attention. This research was supported by grants from the Natural Sciences and Engineering Council of Canada and the Atmospheric Environment Service.

References

Andreae, M. O., Biomass burning: Its history, use, and distribution and its impact on environmental quality and global climate, in Global Biomass Burning: Atmospheric, Climatic, and Biospheric Implications, edited by J. S. Levine, pp. 3-21, MIT Press, Cambridge, Mass., 1991.

Andreae, M. O., et al., Influence of plumes from biomass burning on atmospheric chemistry over the equatorial and tropical South Atlantic during CITE 3, J. Geophys. Res., 99, 12,793-12,808, 1994.

Bachmeier, A. S., et al., PEM-West A: Meteorological overview, J. Geophys. Res., 101, 1655-1677, 1996.

Baumgardner, D., et al., Refractive indices of aerosols in the upper troposphere and lower stratosphere, Geophys. Res. Lett., , 23, 749-752, 1996.

Chatfield, R. B., and P. J. Crutzen, Sulfur dioxide in remote oceanic air: Cloud transport of reactive precursors, J. Geophys. Res., 89, 7111-7132, 1984.

Chatfield, R. B., and A. C. Delany, Convection links biomass burning to increased tropical ozone: However, models will tend to overpredict O_3, J. Geophys. Res., 95, 18,473-18,488, 1990.

Connors, V. S., Savannah burning and convective mixing in southern Africa: Implications for CO emissions and transport, in Global Biomass Burning: Atmospheric, Climatic, and Biospheric Implications, edited by J. S. Levine, pp. 147-154, MIT Press, Cambridge, Mass., 1991.

Connors, V. S., et al., Global distribution of biomass burning and carbon monoxide in the middle troposphere during early April and October 1994, in Biomass Burning and Global Change, vol. 1, Remote Sensing and Modeling of Biomass Burning, and Biomass Burning in the Boreal Forest, edited by J. S. Levine, MIT Press, Cambridge, Mass., 1997.

Crutzen, P. J., and M. O. Andreae, Biomass burning in the tropics: Impact on atmospheric chemistry and biogeochemical cycles, Science, 250, 1669-1678, 1990.

Danielsen, E. F., In situ evidence of rapid, vertical, irreversible transport of lower tropospheric air into the lower tropical stratosphere by convective cloud turrets and by larger-scale upwelling in tropical cyclones, J. Geophys. Res., 98, 8665-8681, 1993.

Danielsen, E. F., et al., Meteorological context for fall experiments including distributions of water vapor, ozone, and carbon monoxide, J. Geophys. Res., 92, 1986-1994, 1987.

Davis, D. D., et al., Assessment of ozone photochemistry in the western North Pacific as inferred from PEM-West A observations during the fall of 1991, J. Geophys. Res., 101, 2111-2134, 1996.

Dickerson, R. R., et al., Thunderstorms: An important mechanism in the transport of air pollutants, Science, 235, 460-465, 1987.

Fahey, D. W., et al. Insitu measurements of total reactive nitrogen, total water, and aerosol in polar stratospheric clouds in the Antarctic stratosphere, J. Geophys. Res., 94, 11,299-11,315, 1989.

Fishman, J., et al., Vertical profiles of ozone, carbon monoxide, and dew point temperature obtained during GTE/-CITE 1, October - November 1983, J. Geophys. Res., 92, 2083-2094, 1987.

Fishman, J., C. E. Watson, J. C. Larsen, and J. A. Logan, Distribution of tropospheric ozone determined from satellite data, J. Geophys. Res., 95, 3599-3617, 1990.

Folkins, I., et al., O_3, NO_y, and NO_x/NO_y in the upper troposphere of the equatorial Pacific, J. Geophys. Res., 100, 20,913-20,926, 1995.

Fu, Q., and K. N. Liou, On the correlated k - distribution method for radiative transfer in nonhomogeneous atmospheres, J. Atmos. Sci., 49, 2139-2156, 1992.

Fujiwara, M. et al., Total ozone enhancement in September and October 1994 in Indonesia, paper presented at the XVIII Quadrennial Ozone Symposium, International Ozone Commission, L'Aquila, Italy, 1996.

Giorgi, F., and W. L. Chameides, Rainout lifetimes of highly soluble aerosols and gases as inferred from simulations with a general circulation model, J. Geophys. Res., 91, 14367-14376, 1986.

Goldammer, J. G., B. Seibert, and W. Schindele, Fire in dipterocarp forests, in Dipterocarp Forest Ecosystems, edited by A. Schulte and D. Schone, pp. 155-185, World Sci., River Edge, N. J., 1996.

Heikes, B. G., et al., Hydrogen Peroxide and methylhydroperoxide distributions related to ozone and odd hydrogen over the North Pacific in the fall of 1991, J. Geophys. Res., 101, 1891-1905, 1996.

Holton, J. R., et al., Stratosphere-troposphere exchange, Rev. Geophys., 33, 403-439, 1995.

Kelly, K. K., et al., A comparison of ER-2 measurements of stratospheric water vapor between the 1987 Antarctic and 1989 Arctic airborne missions, Geophys. Res. Lett., 17, 465-468, 1990.

Kley, D., P. J. Crutzen, H. G. Smith, H. Vomel, S. J. Oltmans, H Grassl, and V. Ramanathan, Observations of near-zero ozone concentrations over the convective Pacific: Effects on air chemistry, Science, 274, 230-233, 1996.

Komala N., S. Saraspriya, K. Kazuyuki, and T. Ogawa, Tropospheric ozone behavior observed in Indonesia, Atmos. Environ., 30, 1851-1856, 1996.

Kousky, V. E., Climate diagnostics bulletin October 1994, U.S. Dep. of Commerce, Washington, D. C., 1994.

Lacis, A. A., D. J. Wuebbles, and J. A. Logan, Radiative forcing of climate by changes in the vertical distribution of ozone, J. Geophys. Res., 95, 9971-9982, 1990.

Liou, K. N., Q. Fu, and T. P. Ackerman, A simple formulation of the δ - four - stream approximation for radiative transfer parameterizations, J. Atmos. Sci., 45, 1940-1947, 1988.

Lobert, J. M., Experimental evaluation of biomass burning emissions: Nitrogen and carbon containing compounds, in Global Biomass Burning: Atmospheric, Climatic, and Biospheric Implications, edited by J. S. Levine, pp. 289-304, MIT Press, Cambridge, Mass., 1991.

Loewenstein, M., et al., New observations of the NO_y/N_2O correlation in the lower stratosphere, Geophys. Res. Lett., 20, 2531-2534, 1993.

Logan, J. A., and V. W. J. H. Kirchhoff, Seasonal variations of tropospheric ozone at Natal, Brazil, J. Geophys. Res., 91, 7875-7881, 1986.

Malingreau, J. P., G. Stevens, and L. Fellows, Remote sensing of forest fires: Kalimantan and north Borneo in 1982-83, Ambio, 14, 314-320, 1985

McFarland, M., D. Kley, J. W. Drummond, A. L. Schmeltekopf, and R. H. Winkler, Nitric oxide measurements in the equatorial Pacific region, Geophys. Res. Lett., 6, 605-608, 1979.

Murphy, D. M., et al., Reactive nitrogen and its correlation with ozone in the lower stratosphere and upper troposphere, J. Geophys. Res., 98, 8751-8773, 1993.

Newell, R. E., et al., Vertical fine-scale atmospheric structure measured from the NASA DC-8 during PEM-West A, J. Geophys. Res., 101, 1943-1960, 1996.

Pickering, K. E., A. M. Thompson, R. R. Dickerson, W. T. Luke, D. P. McNamara, J. Greenberg, and P. R. Zimmerman, Model calculations of tropospheric ozone production potential following observed convective events, J. Geophys. Res., 95, 14,049-14,062, 1990.

Pickering, K. E., J. R. Scala, A. M. Thompson, W. K. Tao, and J. Simpson, A regional estimate of convective transport of CO from biomass burning, Geophys. Res. Lett., 19, 289-292, 1992.

Pickering, K. E., et al., Convective transport of biomass burning emissions over Brazil during TRACE A, J. Geophys. Res., 101, 23993-24012, 1996.

Podolske, J. R., and M. Loewenstein, Airborne tunable diode laser spectrometer for trace-gas measurements in the lower stratosphere, Appl. Opt., 32, 5324-5333, 1993.

Proffitt, M. H., et al., In situ ozone measurements within the 1987 Antarctic ozone hole from a high altitude ER-2 aircraft, J. Geophys. Res., 94, 16,547-16,555, 1989.

Ridley, B. A., M. A. Carroll, and G. L. Gregory, Measurements of nitric oxide in the boundary layer and free troposphere over the Pacific ocean, J. Geophys. Res., 92, 2025-2047, 1987.

Routhier, F., and D. D. Davis, Free tropospheric/boundary-layer airborne measurements of H_2O over the latitude range of 58°S to 70°N: Comparison with simultaneous ozone and carbon dioxide measurements, J. Geophys. Res., 85, 7293-7306, 1980.

Schoeberl, M. R., and L. C. Sparling, Trajectory modeling, in Diagnostic Tools in Atmospheric Physics, Proc. S. I. F. Course CXVI, edited by G. Fiocco and G. Visconti, pp. 289-305, North-Holland, New York, 1994.

Singh, H. B., et al., Reactive nitrogen and ozone over the western Pacific: Distribution, partitioning, and sources, J. Geophys. Res., 101, 1793-1808, 1996.

Thompson, A. M., K. E. Pickering, D. P. McNamara, M. R. Schoeberl, R. D. Hudson, J. H. Kim, E. V. Browell, V. W. J. H. Kirchhoff, and D. Nganga, Where did tropospheric ozone over southern Africa and the tropical Atlantic come from in October 1992? Insights from TOMS, GTE TRACE A, and SAFARI 1992, J. Geophys. Res., 101, 24251-24278, 1996.

Tuck, A. F., Production of nitrogen oxides by lightning discharges, Q. J. R. Meteorol. Soc., 102, 749-755, 1976.

Tuck. A. F. et al., The Brewer Dobson circulation in the light of high altitude in situ aircraft observations, Q. J. R. Meteorol. Soc., in press, 1997.

Webster, C. R., et al., Chlorine chemistry on polar stratospheric cloud particles in the Arctic winter, Science, 261, 1130-1133, 1993.

Webster, C. R., R. D. May, C. A. Trimble, R. G. Chave, and J. Kendall, Aircraft laser infrared absorption (ALIAS) for in situ stratospheric measurements of HCl, N_2O, CH_4, NO_2, and HNO_3, Appl. Opt., 33, 454-472, 1994.

D. Baumgardner, NCAR/RAF, Box 3000, Boulder, CO 80307. (e-mail: darrel@ncar.ucar.edu)

R. Chatfield, Earth System Science Division, NASA Ames Research Center: MS 245-5, Moffett Field, CA 94035. (e-mail: chatfield@clio.arc.nasa.gov)

I. Folkins, Department of Oceanography, Dalhousie University, Halifax, Nova Scotia, Canada, B3H 4J1. (e-mail: folkins@atm.dal.ca)

M. Proffitt, R/E/AL5, NOAA Aeronomy Laboratory, 325 Broadway, Boulder, CO 80303-3328. (e-mail: proffitt@al.noaa.gov)

(Received July 8, 1996; revised December 2, 1996; accepted December 4, 1996.)